

POR

EGG-SEMI-5919

June 1982

EXPERIMENT DATA REPORT FOR THE L9-3

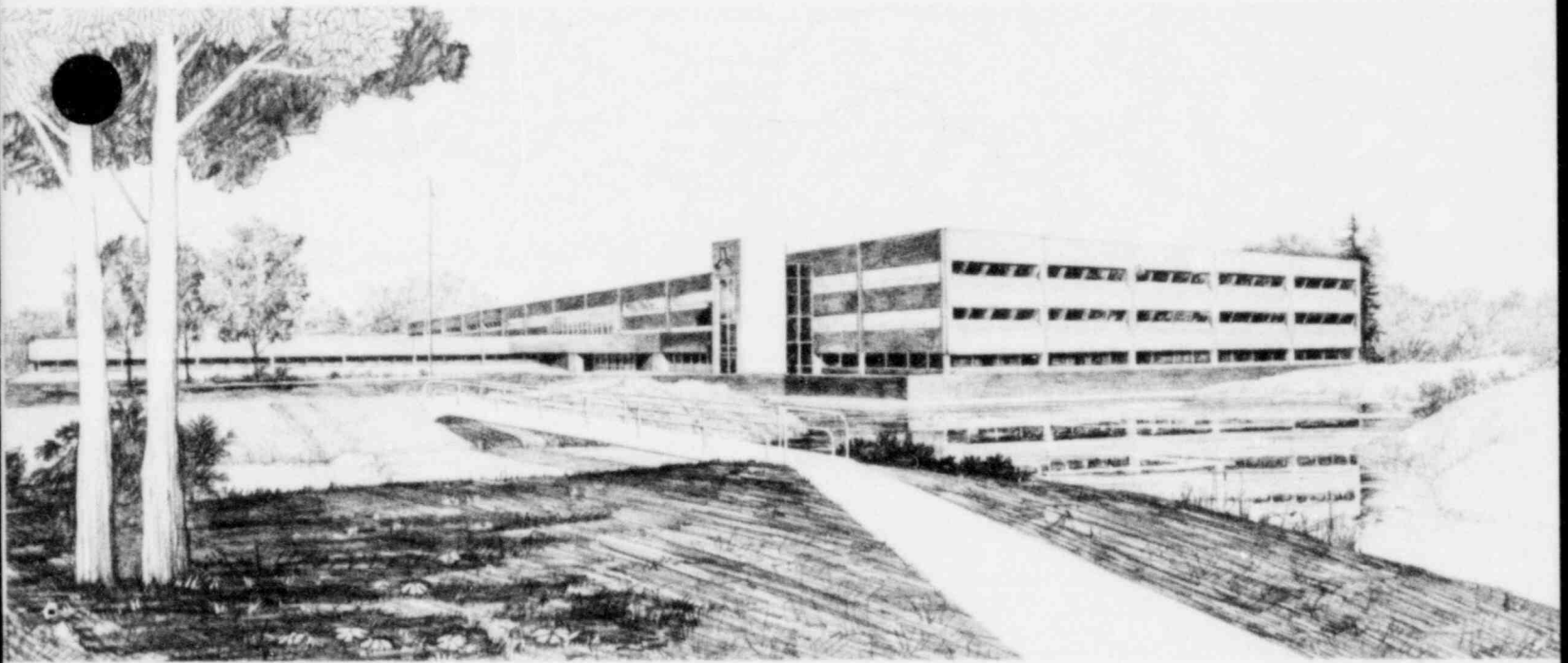
EXPERIMENTAL PORV CALIBRATION TESTS

NRC Research and/or Technical Assistance Rept

W. A. OWCA

U.S. Department of Energy

Idaho Operations Office • Idaho National Engineering Laboratory



This is an informal report intended for use as a preliminary or working document

Prepared for the U.S. Nuclear
Regulatory Commission under DOE
Contract No. DE-AC07-76ID01570
FIN. No. A6038

 **EG&G** Idaho

8208110008 B20630
PDR RES
8208110008 PDR



FORM EG&G-398
(Rev. 11-79)

INTERIM REPORT

Accession No. _____

Report No. EGG-SEMI-5919

Contract Program or Project Title: LOFT Test Support Facility

Subject of this Document: Experimental Data Report for the L9-3 Experimental
PORV Calibration Tests

Type of Document: Experiment Data Report

Author(s): W. A. Owca

Date of Document: June 1982

Responsible NRC Individual and NRC Office or Division: R. R. Landry
Reactor Safety Research

This document was prepared primarily for preliminary or internal use. It has not received full review and approval. Since there may be substantive changes, this document should not be considered final.

EG&G Idaho, Inc.
Idaho Falls, Idaho 83415

Prepared for the
U.S. Nuclear Regulatory Commission
Washington, D.C.
Under DOE Contract No. DE-AC07-76ID01570
NRC FIN No. A6038

INTERIM REPORT

EXPERIMENT DATA REPORT

FOR

THE L9-3 EXPERIMENTAL PORV CALIBRATION TESTS

by

W. A. Owca

Approval:

J. L. Perryman for G.W.J.

G. W. Johnsen, Manager
WRRTF Experiment Planning
and Analysis Branch

Approval:

Paul North

P. North, Manager
Water Reactor Research
Test Facilities Division

ABSTRACT

This report presents the data from the LOFT L9-3 experimental pressure operated relief valve (PORV) and code safety valve, test series conducted in the Blowdown Facility at the LOFT Test Support Facility (LTSF). The objectives of the tests were to size the valve to pass specified mass flow rates of saturated steam at specified upstream conditions, and to determine the mass flow rate of subcooled liquid through the valve at the combined PORV and code safety valve setting. Calibration data were successfully obtained and are presented here in uninterpreted form.

SUMMARY

The LOFT program is designed to provide a data base for safety research on loss-of-coolant accidents and operational transients in a pressurized water reactor (PWR). The LOFT L9-3 experiment was intended to simulate PWR behavior under Anticipated Transient Without Scram (ATWS) conditions, specifically a loss of feedwater initiated transient without scram. The pressure operated relief valve (PORV) was required to mitigate the pressure rise by passing specified mass flow rates of steam and subcooled liquid. The L9-3 PORV Calibration Testing at LTSF was required to size the valve to pass specified mass flow rates of saturated steam, and to determine the subcooled mass flow rate through the valve at the calibrated setting. The L9-3 PORV testing was conducted in the Blowdown Facility located in the LOFT Test Support Facility at the Idaho National Engineering Laboratory during February and March 1982.

The Blowdown Facility basically consists of a 277-L (73 gallon) pressure vessel, a catch tank suspended on load cells and associated piping which connects the pressure vessel to the catch tank. Heater rods, pumps and additional piping are provided so that the system can be heated and pressurized to a variety of temperatures and pressures. Reference instrumentation includes pressure and temperature measurements, a gamma densitometer, and the catch tank load cells which measure the mass of fluid discharged into the catch tank as a function of time. The data from these transducers were collected and recorded on a Mod Comp II/45 computer.

The L9-3 valve calibration test data were produced successfully and are stored on the Cyber computer system for future reference. The data are presented here in uninterpreted form.

The PORV was successfully sized to pass the specified mass flow rate of saturated steam. In addition, subcooled discharge rates were determined for various degrees of subcooling.

CONTENTS

ABSTRACT	ii
SUMMARY	iii
1. INTRODUCTION	1
2. SYSTEM PROCEDURES, CONDITIONS, AND EVENTS FOR THE L9-3 PORV CALIBRATION TESTING	3
2.1 System Configuration	3
2.2 Instrumentation	3
2.3 Test Preparation and Warm-Up	4
2.4 Test Sequence	5
3. DATA PRESENTATION	6
4. REFERENCES	7
APPENDIX A--CATCH TANK CALIBRATION	11
APPENDIX B--UNCERTAINTY ANALYSIS	17
APPENDIX C--DATA PROCESSING AND QUALIFICATION	21
APPENDIX D--DATA ACQUISITION SYSTEM	25

TABLES

1. L9-3 experimental PORV test instrumentation	30
2. L9-3 experimental PORV test data summary	32

FIGURES

1. L9-3 experimental PORV test facility isometric	8
2. L9-3 experimental PORV	9
3. L9-3 experimental PORV test instruments	10

NOTE: Figures 4 through 276 are presented on microfiche attached to inside of the back cover.

Test BF-L9-3-1B

4. Densitometer, bottom beam, upstream of the PORV (DE-1A)
5. Densitometer, top beam, upstream of the PORV (DE-1B)
6. Fluid temperature in the pressure vessel (BF-TE-5)
7. Fluid temperature upstream of the PORV (TE-PORV-1)
8. Fluid temperature downstream of the PORV (TE-PORV-2)
9. Fluid temperature upstream of the reference orifice (TE-0-1)
10. Pressure upstream of the PORV (PE-PORV-1)
11. Pressure downstream of the PORV (PE-PORV-2)
12. Liquid level in the pressure vessel (BF-PDE-23)
13. Pressure in the pressure vessel (BF-PE-3)
14. Differential pressure across the PORV (PDE-PORV)
15. Pressure upstream of the reference orifice (PE-0-1)
16. North load cell (LD-LC-2)
17. South load cell (LD-LC-1)
18. Differential pressure from reference orifice to PORV
(PDE-REF)

Test BF-L9-3-1C

19. Densitometer, bottom beam, upstream of the PORV (DE-1A)
20. Densitometer, top beam, upstream of the PORV (DE-1B)
21. Fluid temperature in the pressure vessel (BF-TE-5)
22. Fluid temperature upstream of the PORV (TE-PORV-1)
23. Fluid temperature downstream of the PORV (TE-PORV-2)
24. Fluid temperature upstream of the reference orifice (TE-0-1) .. .
25. Pressure upstream of the PORV (PE-PORV-1)
26. Pressure downstream of the PORV (PE-PORV-2)
27. Liquid level in the pressure vessel (BF-PDE-23)

- 28. Pressure in the pressure vessel (BF-PE-3)
- 29. Differential pressure across the PORV (PDE-PORV)
- 30. Pressure upstream of the reference orifice (PE-0-1)
- 31. North load cell (LD-LC-2)
- 32. South load cell (LD-LC-1)
- 33. Differential pressure from reference orifice to PORV
(PDE-REF)
- Test BF-L9-3-1D
- 34. Densitometer, bottom beam, upstream of the PORV (DE-1A)
- 35. Densitometer, top beam, upstream of the PORV (DE-1B)
- 36. Fluid temperature in the pressure vessel (BF-TE-5)
- 37. Fluid temperature upstream of the PORV (TE-PORV-1)
- 38. Fluid temperature downstream of the PORV (TE-PORV-2)
- 39. Fluid temperature upstream of the reference orifice (TE-0-1)
- 40. Pressure upstream of the PORV (PE-PORV-1)
- 41. Pressure downstream of the PORV (PE-PORV-2)
- 42. Liquid level in the pressure vessel (BF-PDE-23)
- 43. Pressure in the pressure vessel (BF-PE-3)
- 44. Differential pressure across the PORV (PDE-PORV)
- 45. Pressure upstream of the reference orifice (PE-0-1)
- 46. North load cell (LD-LC-2)
- 47. South load cell (LD-LC-1)
- 48. Differential pressure from reference orifice to PORV
(PDE-REF)
- Test BF-L9-3-1E
- 49. Densitometer, bottom beam, upstream of the PORV (DE-1A)
- 50. Densitometer, top beam, upstream of the PORV (DE-1B)
- 51. Fluid temperature in the pressure vessel (BF-TE-5)

52.	Fluid temperature upstream of the PORV (TE-PORV-1)	
53.	Fluid temperature downstream of the PORV (TE-PORV-2)	
54.	Fluid temperature upstream of the reference orifice (TE-0-1)	
55.	Pressure upstream of the PORV (PE-PORV-1)	
56.	Pressure downstream of the PORV (PE-PORV-2)	
57.	Liquid level in the pressure vessel (BF-PDE-23)	
58.	Pressure in the pressure vessel (BF-PE-3)	
59.	Differential pressure across the PORV (PDE-PORV)	
60.	Pressure upstream of the reference orifice (PE-0-1)	
61.	North load cell (LD-LC-2)	
62.	South load cell (LD-LC-1)	
63.	Differential pressure from reference orifice to PORV (PDE-REF)	
	Test BF-L9-3-1ER	
64.	Densitometer, bottom beam, upstream of the PORV (DE-1A)	
65.	Densitometer, top beam, upstream of the PORV (DE-1B)	
66.	Fluid temperature in the pressure vessel (BF-TE-5)	
67.	Fluid temperature upstream of the PORV (TE-PORV-1)	
68.	Fluid temperature downstream of the PORV (TE-PORV-2)	
69.	Fluid temperature upstream of the reference orifice (TE-0-1)	
70.	Pressure upstream of the PORV (PE-PORV-1)	
71.	Pressure downstream of the PORV (PE-PORV-2)	
72.	Liquid level in the pressure vessel (BF-PDE-23)	
73.	Pressure in the pressure vessel (BF-PE-3)	
74.	Differential pressure across the PORV (PDE-PORV)	
75.	Pressure upstream of the reference orifice (PE-0-1)	
76.	North load cell (LD-LC-2)	

- 77. South load cell (LD-LC-1)
- 78. Differential pressure from reference orifice to PORV
(PDE-REF)
- Test BF-L9-3-2A
- 79. Densitometer, bottom beam, upstream of the PORV (DE-1A)
- 80. Densitometer, top beam, upstream of the PORV (DE-1B)
- 81. Fluid temperature in the pressure vessel (BF-TE-5)
- 82. Fluid temperature upstream of the PORV (TE-PORV-1)
- 83. Fluid temperature downstream of the PORV (TE-PORV-2)
- 84. Fluid temperature upstream of the reference orifice (TE-0-1)
- 85. Pressure upstream of the PORV (PE-PORV-1)
- 86. Pressure downstream of the PORV (PE-PORV-2)
- 87. Liquid level in the pressure vessel (BF-PDE-23)
- 88. Pressure in the pressure vessel (BF-PE-3)
- 89. Differential pressure across the PORV (PDE-PORV)
- 90. Pressure upstream of the reference orifice (PE-0-1)
- 91. North load cell (LD-LC-2)
- 92. South load cell (LD-LC-1)
- 93. Differential pressure from reference orifice to PORV
(PDE-REF)
- Test BF-L9-3-2B
- 94. Densitometer, bottom beam, upstream of the PORV (DE-1A)
- 95. Densitometer, top beam, upstream of the PORV (DE-1B)
- 96. Fluid temperature in the pressure vessel (BF-TE-5)
- 97. Fluid temperature upstream of the PORV (TE-PORV-1)
- 98. Fluid temperature downstream of the PORV (TE-PORV-2)
- 99. Fluid temperature upstream of the reference orifice (TE-0-1)
- 100. Pressure upstream of the PORV (PE-PORV-1)

101.	Pressure downstream of the PORV (PE-PORV-2)	
102.	Liquid level in the pressure vessel (BF-PDE-23)	
103.	Pressure in the pressure vessel (BF-PE-3)	
104.	Differential pressure across the PORV (PDE-PORV)	
105.	Pressure upstream of the reference orifice (PE-0-1)	
106.	North load cell (LD-LC-2)	
107.	South load cell (LD-LC-1)	
108.	Differential pressure from reference orifice to PORV (PDE-REF)	
	Test BF-L9-3-2C	
109.	Densitometer, bottom beam, upstream of the PORV (DE-1A)	
110.	Densitometer, top beam, upstream of the PORV (DE-1B)	
111.	Fluid temperature in the pressure vessel (BF-TE-5)	
112.	Fluid temperature upstream of the PORV (TE-PORV-1)	
113.	Fluid temperature downstream of the PORV (TE-PORV-2)	
114.	Fluid temperature upstream of the reference orifice (TE-0-1)	
115.	Pressure upstream of the PORV (PE-PORV-1)	
116.	Pressure downstream of the PORV (PE-PORV-2)	
117.	Liquid level in the pressure vessel (BF-PDE-23)	
118.	Pressure in the pressure vessel (BF-PE-3)	
119.	Differential pressure across the PORV (PDE-PORV)	
120.	Pressure upstream of the reference orifice (PE-0-1)	
121.	North load cell (LD-LC-2)	
122.	South load cell (LD-LC-1)	
123.	Differential pressure from reference orifice to PORV (PDE-REF)	

Test BF-L9-3-2D

- 124. Densitometer, bottom beam, upstream of the PORV (DE-1A)
- 125. Densitometer, top beam, upstream of the PORV (DE-1B)
- 126. Fluid temperature in the pressure vessel (BF-TE-5)
- 127. Fluid temperature upstream of the PORV (TE-PORV-1)
- 128. Fluid temperature downstream of the PORV (TE-PORV-2)
- 129. Fluid temperature upstream of the reference orifice (TE-0-1)
- 130. Pressure upstream of the PORV (PE-PORV-1)
- 131. Pressure downstream of the PORV (PE-PORV-2)
- 132. Liquid level in the pressure vessel (BF-PDE-23)
- 133. Pressure in the pressure vessel (BF-PE-3)
- 134. Differential pressure across the PORV (PDE-PORV)
- 135. Pressure upstream of the reference orifice (PE-0-1)
- 136. North load cell (LD-LC-2)
- 137. South load cell (LD-LC-1)
- 138. Differential pressure from reference orifice to PORV
(PDE-REF)

Test BF-L9-3-2E

- 139. Densitometer, bottom beam, upstream of the PORV (DE-1A)
- 140. Densitometer, top beam, upstream of the PORV (DE-1B)
- 141. Fluid temperature in the pressure vessel (BF-TE-5)
- 142. Fluid temperature upstream of the PORV (TE-PORV-1)
- 143. Fluid temperature downstream of the PORV (TE-PORV-2)
- 144. Fluid temperature upstream of the reference orifice (TE-0-1)
- 145. Pressure upstream of the PORV (PE-PORV-1)
- 146. Pressure downstream of the PORV (PE-PORV-2)
- 147. Liquid level in the pressure vessel (BF-PDE-23)

148.	Pressure in the pressure vessel (BF-PE-3)	
149.	Differential pressure across the PORV (PDE-PORV)	
150.	Pressure upstream of the reference orifice (PE-0-1)	
151.	North load cell (LD-LC-2)	
152.	South load cell (LD-LC-1)	
153.	Differential pressure from reference orifice to PORV (PDE-REF)	
	Test BF-L9-3-2F	
154.	Densitometer, bottom beam, upstream of the PORV (DE-1A)	
155.	Densitometer, top beam, upstream of the PORV (DE-1B)	
156.	Fluid temperature in the pressure vessel (BF-TE-5)	
157.	Fluid temperature upstream of the PORV (TE-PORV-1)	
158.	Fluid temperature downstream of the PORV (TE-PORV-2)	
159.	Fluid temperature upstream of the reference orifice (TE-0-1)	
160.	Pressure upstream of the PORV (PE-PORV-1)	
161.	Pressure downstream of the PORV (PE-PORV-2)	
162.	Liquid level in the pressure vessel (BF-PDE-23)	
163.	Pressure in the pressure vessel (BF-PE-3)	
164.	Differential pressure across the PORV (PDE-PORV)	
165.	Pressure upstream of the reference orifice (PE-0-1)	
166.	North load cell (LD-LC-2)	
167.	South load cell (LD-LC-1)	
168.	Differential pressure from reference orifice to PORV (PDE-REF)	
	Test BF-L9-3-2G	
169.	Densitometer, bottom beam, upstream of the PORV (DE-1A)	
170.	Densitometer, top beam, upstream of the PORV (DE-1B)	
171.	Fluid temperature in the pressure vessel (BF-TE-5)	

172.	Fluid temperature upstream of the PORV (TE-PORV-1)	
173.	Fluid temperature downstream of the PORV (TE-PORV-2)	
174.	Fluid temperature upstream of the reference orifice (TE-0-1)	
175.	Pressure upstream of the PORV (PE-PORV-1)	
176.	Pressure downstream of the PORV (PE-PORV-2)	
177.	Liquid level in the pressure vessel (BF-PDE-23)	
178.	Pressure in the pressure vessel (BF-PE-3)	
179.	Differential pressure across the PORV (PDE-PORV)	
180.	Pressure upstream of the reference orifice (PE-0-1)	
181.	North load cell (LD-LC-2)	
182.	South load cell (LD-LC-1)	
183.	Differential pressure from reference orifice to PORV (PDE-REF)	
	Test BF-L9-3-2H	
184.	Densitometer, bottom beam, upstream of the PORV (DE-1A)	
185.	Densitometer, top beam, upstream of the PORV (DE-1B)	
186.	Fluid temperature in the pressure vessel (BF-TE-5)	
187.	Fluid temperature upstream of the PORV (TE-PORV-1)	
188.	Fluid temperature downstream of the PORV (TE-PORV-2)	
189.	Fluid temperature upstream of the reference orifice (TE-0-1)	
190.	Pressure upstream of the PORV (PE-PORV-1)	
191.	Pressure downstream of the PORV (PE-PORV-2)	
192.	Liquid level in the pressure vessel (BF-PDE-23)	
193.	Pressure in the pressure vessel (BF-PE-3)	
194.	Differential pressure across the PORV (PDE-PORV)	
195.	North load cell (LD-LC-2)	
196.	South load cell (LD-LC-1)	

197.	Differential pressure from reference orifice to PORV (PDE-REF)	
	Test BF-L9-3-2HRR	
198.	Densitometer, bottom beam, upstream of the PORV (DE-1A)	
199.	Densitometer, top beam, upstream of the PORV (DE-1B)	
200.	Fluid temperature in the pressure vessel (BF-TE-5)	
201.	Fluid temperature upstream of the PORV (TE-PORV-1)	
202.	Fluid temperature downstream of the PORV (TE-PORV-2)	
203.	Fluid temperature upstream of the reference orifice (TE-0-1)	
204.	Pressure upstream of the PORV (PE-PORV-1)	
205.	Pressure downstream of the PORV (PE-PORV-2)	
206.	Liquid level in the pressure vessel (BF-PDE-23)	
207.	Pressure in the pressure vessel (BF-PE-3)	
208.	Differential pressure across the PORV (PDE-PORV)	
209.	Pressure upstream of the reference orifice (PE-0-1)	
210.	North load cell (LD-LC-2)	
211.	South load cell (LD-LC-1)	
212.	Differential pressure from reference orifice to PORV (PDE-REF)	
	Test BF-L9-3-SC-1	
213.	Densitometer, bottom beam, upstream of the PORV (DE-1A)	
214.	Densitometer, top beam, upstream of the PORV (DE-1B)	
215.	Fluid temperature in the pressure vessel (BF-TE-5)	
216.	Fluid temperature upstream of the PORV (TE-PORV-1)	
217.	Fluid temperature downstream of the PORV (TE-PORV-2)	
218.	Fluid temperature upstream of the reference orifice (TE-0-1)	
219.	Pressure upstream of the PORV (PE-PORV-1)	

220.	Pressure downstream of the PORV (PE-PORV-2)	
221.	Liquid level in the pressure vessel (BF-PDE-23)	
222.	Pressure in the pressure vessel (BF-PE-3)	
223.	Differential pressure across the PORV (PDE-PORV)	
224.	Differential pressure from reference orifice (PDE-FT-1)	
225.	Pressure upstream of the reference orifice (PE-O-1)	
226.	North load cell (LD-LC-2)	
227.	South load cell (LD-LC-1)	
228.	Pressure in Nitrogen injection header (PE-N-1)	
	Test BF-L9-3-SC-2	
229.	Densitometer, bottom beam, upstream of the PORV (DE-1A)	
230.	Densitometer, top beam, upstream of the PORV (DE-1B)	
231.	Fluid temperature in the pressure vessel (BF-TE-5)	
232.	Fluid temperature upstream of the PORV (TE-PORV-1)	
233.	Fluid temperature downstream of the PORV (TE-PORV-2)	
234.	Fluid temperature upstream of the reference orifice (TE-O-1)	
235.	Pressure upstream of the PORV (PE-PORV-1)	
236.	Pressure downstream of the PORV (PE-PORV-2)	
237.	Liquid level in the pressure vessel (BF-PDE-23)	
238.	Pressure in the pressure vessel (BF-PE-3)	
239.	Differential pressure across the PORV (PDE-PORV)	
240.	Differential pressure across the reference flow orifice (PDE-FT-1)	
241.	Pressure upstream of the reference orifice (PE-O-1)	
242.	North load cell (LD-LC-2)	
243.	South load cell (LD-LC-1)	
244.	Pressure in nitrogen injection header (PE-N-1)	

Test BF-L9-3-SC-3

245.	Densitometer, bottom beam, upstream of the PORV (DE-1A)	
246.	Densitometer, top beam, upstream of the PORV (DE-1B)	
247.	Fluid temperature in the pressure vessel (BF-TE-5)	
248.	Fluid temperature upstream of the PORV (TE-PORV-1)	
249.	Fluid temperature downstream of the PORV (TE-PORV-2)	
250.	Fluid temperature upstream of the reference orifice (TE-0-1)	
251.	Pressure upstream of the PORV (PE-PORV-1)	
252.	Pressure downstream of the PORV (PE-PORV-2)	
253.	Liquid level in the pressure vessel (BF-PDE-23)	
254.	Pressure in the pressure vessel (BF-PE-3)	
255.	Differential pressure across the PORV (PDE-PORV)	
256.	Differential pressure across the reference flow orifice (PDE-FT-1)	
257.	Pressure upstream of the reference orifice (PE-0-1)	
258.	North load cell (LU-LC-2)	
259.	South load cell (LD-LC-1)	
260.	Pressure in nitrogen injection header (PE-N-1)	

Test BF-L9-3-SC-4R

261.	Densitometer, bottom beam, upstream of the PORV (DE-1A)	
262.	Densitometer, top beam, upstream of the PORV (DE-1B)	
263.	Fluid temperature in the pressure vessel (BF-TE-5)	
264.	Fluid temperature upstream of the PORV (TE-PORV-1)	
265.	Fluid temperature downstream of the PORV (TE-PORV-2)	
266.	Fluid temperature upstream of the reference orifice (TE-0-1)	
267.	Pressure upstream of the PORV (PE-PORV-1)	
268.	Pressure downstream of the PORV (PE-PORV-2)	

269. Liquid level in the pressure vessel (BF-PDE-23)

270. Pressure in the pressure vessel (BF-PE-3)

271. Differential pressure across the PORV (PDE-PORV)

272. Differential pressure across the reference flow orifice
(PDE-FT-1)

273. Pressure upstream of the reference orifice (PE-0-1)

274. North load cell (LD-LC-2)

275. South load cell (LD-LC-1)

276. Pressure in nitrogen injection header (PE-N-1)

EXPERIMENT DATA REPORT FOR LOFT L9-3 EXPERIMENTAL
PRESSURIZER RELIEF VALVE CALIBRATION TESTING

1. INTRODUCTION

This document describes procedures, hardware, and instrumentation used and presents data produced during the Loss of Fluid Test (LOFT) L9-3 experimental pressurizer relief and code safety valve (PORV) calibration testing at LTSF. The LOFT L9-3 experiment was intended to simulate pressurized water reactor (PWR) behavior under Anticipated Transient Without Scram (ATWS) conditions. The L9-3 experiment was designed to simulate a loss of feedwater initiated transient with failure to SCRAM. The loss of secondary heat sink and subsequent primary fluid expansion causes a pressure increase, and the PORV was required to mitigate the pressure rise by passing a specified mass flow rate of superheated steam, two-phase fluid, and subcooled liquid water.

The PORV used during the LOFT L9-3 experiment simulated both the pressurizer relief and code safety valves. The valve utilized a dual position actuator, simulating relief valve operation (at the low setting), and combined relief and code safety valve operation (at the high setting). Valve performance assessment, and calibration of low and high actuator set points was required prior to installation in LOFT.

The valve testing was performed using the Blowdown Facility (BF) at LTSF. Testing required subcooled liquid flows and saturated steam flows with reference measurements required to determine pressure, temperature, density and mass flow rates.

Objectives of the PORV tests at LTSF were:

1. The PORV was to be sized to pass two specified mass flow rates of saturated steam. The low actuator setting was to simulate the relief valve opening at 2350 psia. The high actuator setting was to simulate the combined relief valve and safety valve opening at 2500 psia.

2. The mass flow rate of subcooled liquid at 2500 psia for the high actuator setting was then to be determined.
3. Valve integrity and performance under high pressure/temperature conditions were to be verified.

The PORV was sized at lower pressures than those specified above. Using the reference mass flow rate from the catch tank, and pressure and temperature upstream of the PORV, the data were extrapolated to provide the mass flow rates of actual LOFT conditions. These tests also provided information to assess the structural integrity and the operational performance of the valve at high pressures and temperatures.

Section 2 of this document describes the system configuration, instrumentation and test conduct. Section 3 presents the test data and supporting information to aid interpretation. Four appendices detail the pretest catch tank calibration, the test data uncertainty, data processing, and the data acquisition system.

2. SYSTEM PROCEDURES, CONDITIONS, AND EVENTS FOR THE L9-3 PORV CALIBRATION TESTING

2.1 System Configuration

The hardware for this test series consisted of the primary BF components, specifically the pressure vessel, warm-up and test heaters, the main pump, and associated valves and piping. Figure 1 shows the system configuration for these tests with control valves identified, and the test specific hardware is detailed in Reference 1. The pressure vessel is constructed of 16-in. schedule 160 pipe, with hemispherical end caps enclosing a maximum fluid volume of 277 L (73 gal). The main coolant pump is a 22 L/s (350 gpm) constant speed pump. The heat-up system consisted of two 1-in. test heater vessels each containing one heater rod, and a 3-in. warm-up heater vessel containing four heater rods. Maximum combined test heaters and warm-up heater power was 111 kW. These loop components were heavily insulated to help maintain isothermal conditions. In addition, a 14-in. spool, a reference metering section, the PORV spool, the catch tank, the nitrogen injection system, and connecting spools and valves were used.

The L9-3 PORV had a standard Valtek body and a double actuator assembly developed by LOFT (Figure 2). The actuators were set prior to testing to provide two different valve openings. The valve could be opened from a shut position to either of the valve settings.

2.2 Instrumentation

A list of instruments used is shown in Table 1. This list consists of measurements of temperature, pressure, differential pressure, density, and mass. Test instrument locations are detailed in Figure 3. Other measurements were made, but only those pertinent to the valve calibration are reported here.

Fluid temperature measurements were made in the pressure vessel (TE-5), in the 14-in. spool piece (TE-SB-2), upstream of the reference mass flow rate orifice (TE-O-1), and upstream and downstream of the PORV (TE-PORV-1,2).

Pressure measurements were made throughout the system including the pressure vessel (PE-3), the 14-in. spool piece (PE-SB-2), upstream of the reference mass flow rate orifice (PE-O-1), upstream and downstream of the PORV (PE-PORV-1,2), and in the Nitrogen Supply line (PE-N-1).

Differential pressure measurements were made across the pressure vessel (PDE-23) to determine the liquid level, across the PORV (PDE-PORV), across the reference mass flow orifice (PDE-FT-1) for the subcooled tests, and from the downstream flange of the reference orifice to the PORV (PDE-REF) for the saturated steam tests.

A density measurement was made using a two-beam densitometer located on the 1-1/2-in. line upstream of the PORV (DE-1A, 1B).

The load cell/catch tank assembly was used to determine the fluid mass that passed through the PORV. This signal was differentiated with respect to time to determine a reference mass flow rate, for the saturated steam tests, and was compared to the orifice meter mass flow rate for the subcooled tests. The reference orifice meter was installed in the metering section for the subcooled tests only. However, the metering section pressure (PE-O-1) and temperature (TE-O-1) were used in all tests.

2.3 Test Preparation and Warm-Up

Prior to each test, the system was filled with treated demineralized water and vented to ensure a liquid-full system. The system was leak-checked and loop components and instruments were performance checked.

The main coolant pump was used to circulate water through the warm-up and test heaters, and the pressure vessel and test piping to heat the loop. A LOFT data average (LDA) was taken at 50 K intervals to assess data

system performance and instrument integrity. The loop was heated so that at test initiation all loop piping and fluid was within ± 5 K of specified conditions.

2.4 Test Sequence

Two types of tests were conducted during this test series, saturated steam blowdowns and steady state, subcooled liquid discharge tests. The EPTAK microprocessor controller was used to control valve lineups, test initiation, pressure control, and test termination for all tests.

The PORV was opened to either the low or high position to initiate saturated steam blowdowns. The system pressure dropped immediately to saturation, and subsequent depressurization resulted in boiling with saturated steam produced at the top of the pressure vessel. The steam flow path was from the top of the pressure vessel through CV-1T, the densitometer spool, the PORV and into the catch tank (see Figure 1). This method of operation produced saturated steam conditions upstream of the PORV at pressures of 3.4 to 10.0 MPa, (500 to 1450 psia) depending upon mass flow rate, and initial system temperature.

Subcooled blowdowns were initiated by opening the PORV to the high position. Constant pressure was maintained by nitrogen injection at the top of the pressure vessel. The nitrogen flow control valve (NS-FCV-14) was automatically controlled using a signal from a pressure transducer at the top of the pressure vessel. The subcooled liquid flow path was from the bottom of the pressure vessel, through the 14-in. spool, upwards through CV-2T, the densitometer spool, the PORV, and into the catch tank. Varying degrees of subcooling, from 3 to 30 K, were produced by maintaining constant pressure and varying the fluid temperature for different tests. This method of operation produced steady state, subcooled liquid conditions upstream of the PORV for a minimum 20 s test interval.

3. DATA PRESENTATION

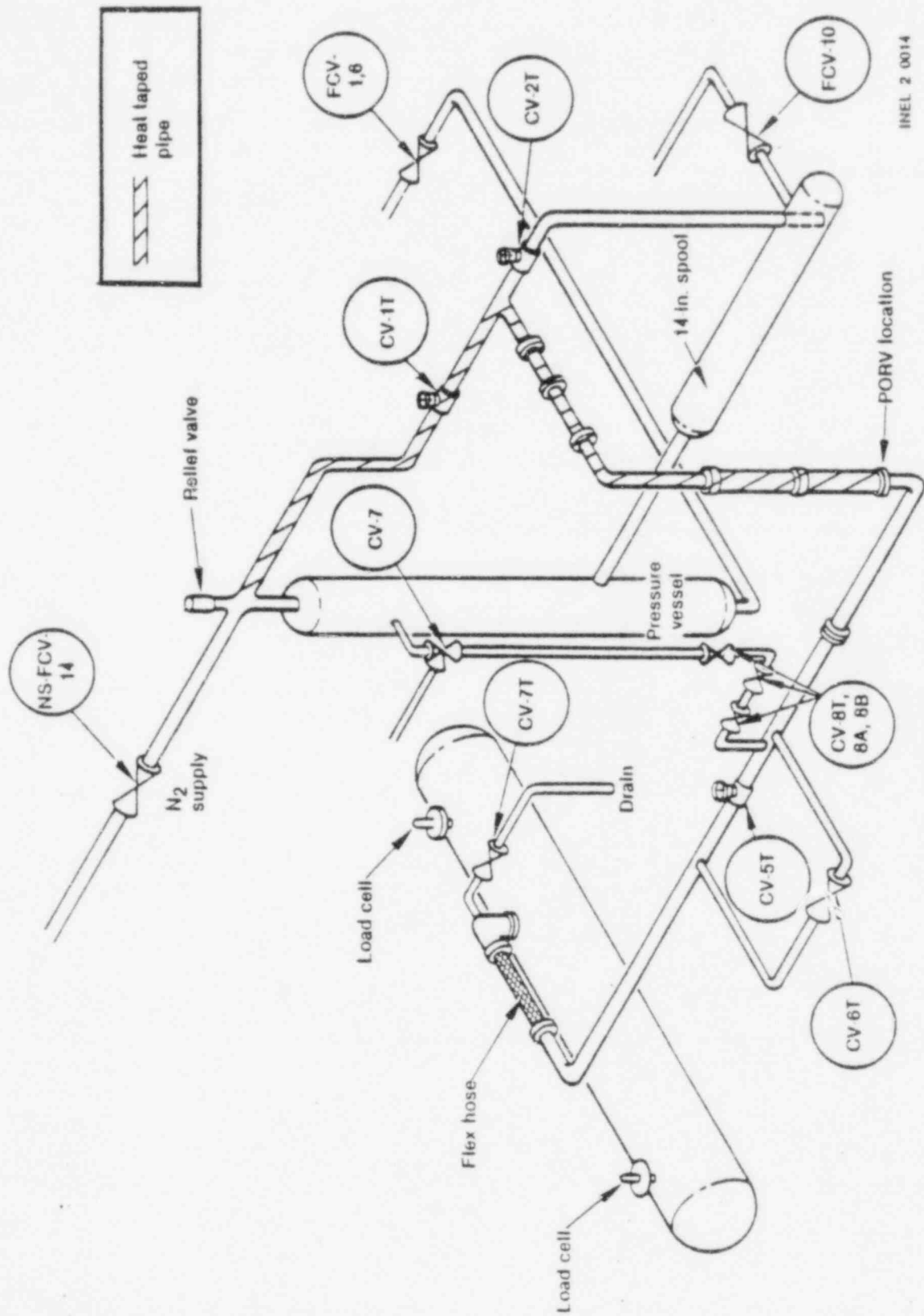
The measurements obtained from the PORV calibration tests are listed in Table 1, with transducer location and applicable range. Table 2 details the test conditions for each data point. Test initiation conditions are the steady state conditions achieved immediately prior to opening the test valve. The pressure range and temperature range tabulated are the conditions at which saturated steam was present upstream of the PORV for the saturated steam tests and during steady state conditions for the subcooled tests. Test type is designated as SC for subcooled tests, and SAT for saturated steam tests. Valve setting is specified as H for high actuator, combined valve setting, or L for low actuator, PORV setting. Valve opening is listed as percent of full stem travel.

The L9-3 PORV calibration test data tapes can be accessed on the INEL Cyber computer system under the permanent file ID NLNLSF. The permanent file name for each test is the same as the test ID in Table 2.

The data plots are presented in Figures 4 through 281 on microfiche contained on the back cover of this report. The transducer ID, test ID, and uncertainty are listed. The data have been processed to provide engineering unit versus time plots. Data spikes exist on most of the plots. These spikes are produced by noise in the data acquisition system (DAS) and are not real test data. The plots have been scaled to best present the data by ignoring the noise spikes where necessary. Appendix A summarizes the catch tank calibration preceding the test series. The measurement uncertainty analysis is detailed in Appendix B, and the data reduction methods and qualification are detailed in Appendix C. The data acquisition system is described in Appendix D.

REFERENCES

1. Drawing Number 415432, LTSF L9-3/4 Test Apparatus Assembly, Release date 12-9-81.
2. W. A. Owca, Experiment Operating Specification for LOFT L9-3 Experimental Pressurizer Relief Valve Calibration Testing, EGG-SEMI-5773, February 1982.



INEL 2 0014

Figure 1. L9-3 experimental PORV test facility isometric.

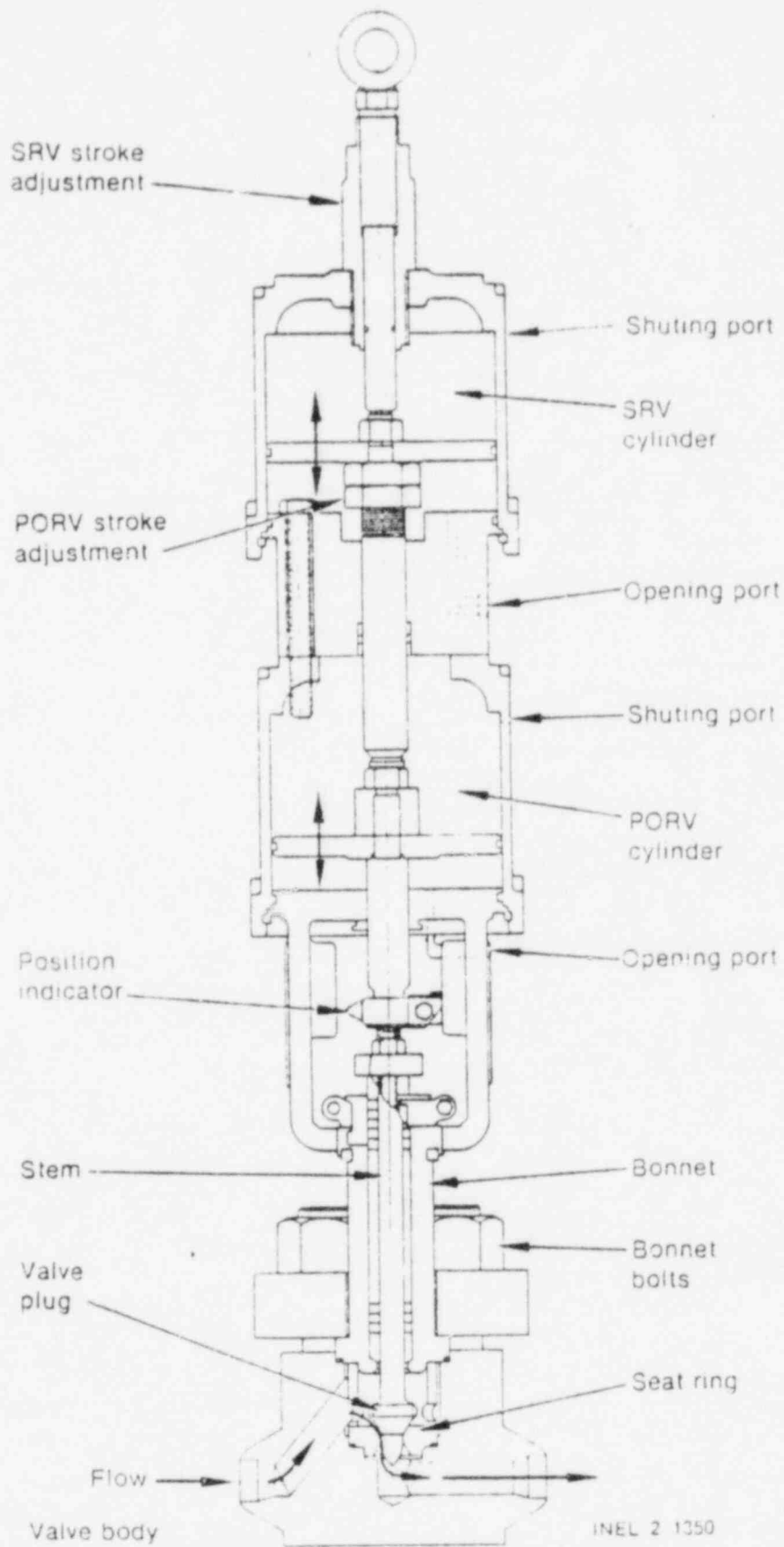
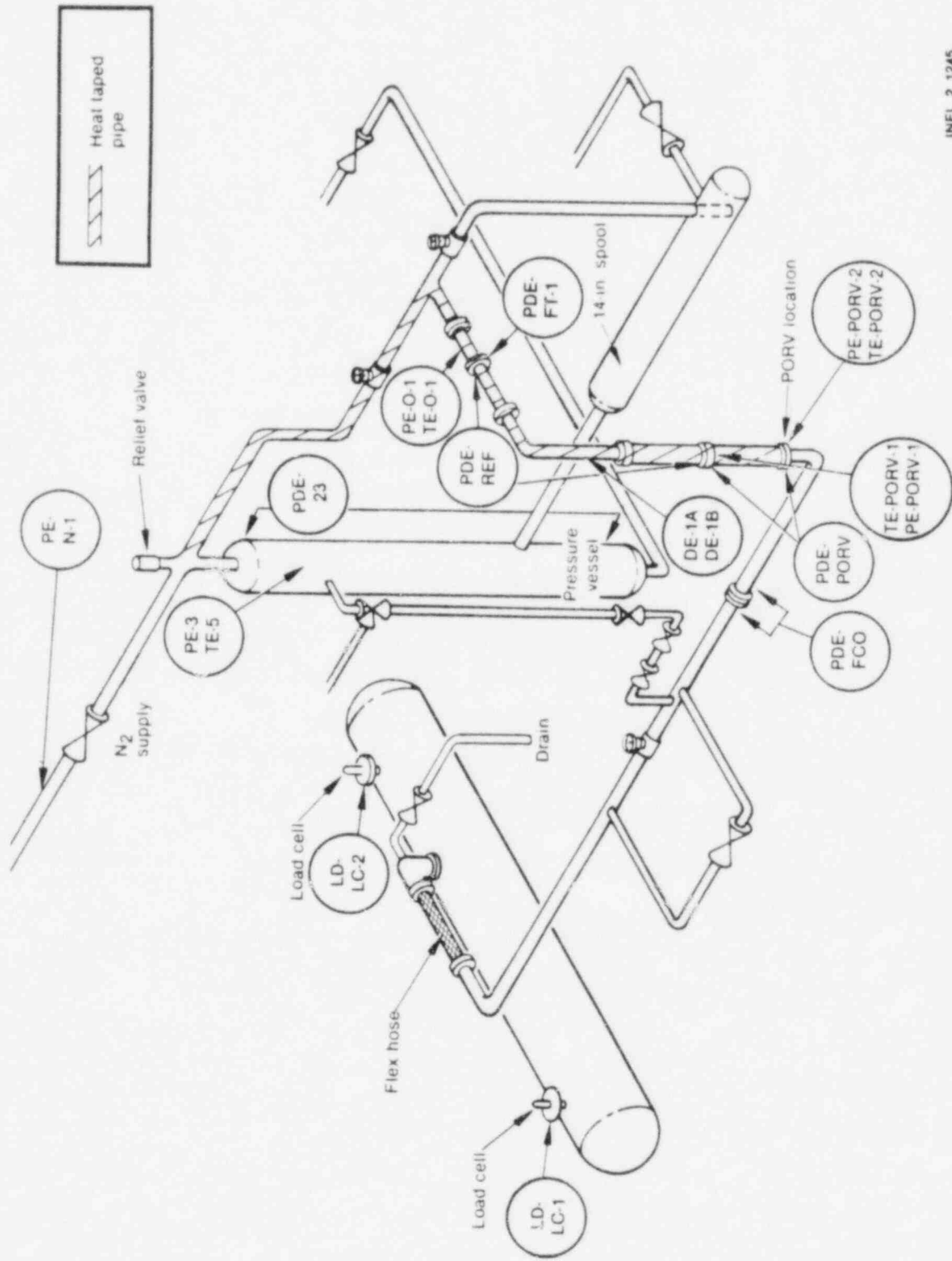


Figure 2. L9-3 Experimental PORV.



INEL 2 1245

Figure 3. L9-3 Experimental PORV test instruments.

APPENDIX A

CATCH TANK CALIBRATION

APPENDIX A

CATCH TANK CALIBRATION

Introduction

A catch tank calibration was conducted prior to the L9-3 PORV test series. The objectives of the calibration tests were to determine the accuracy of the weighing system, to provide information on the weighing system uncertainty, and to determine response characteristics of the catch tank-load cell assembly to transient type tests.^{A-1} This appendix describes the tests and results obtained.

System Procedures, Conditions and Events

System Configuration

The system configuration was very similar to that used for the L9-3 valve calibration. The PORV spool was replaced by a 1-in. schedule 160, replacement spool. A flow control orifice was placed between the PORV spool and CV-5T (see Figure 2). Two different orifices were used to produce mass flow rates intended to approximate the ranges expected in the L9-3 PORV test series. A flow straightener^{A-2} installed in the flex hose at the catch tank inlet, for the L9-3 valve testing, was not installed during the catch tank calibration tests.

Instrumentation

Measurements made during the catch tank calibration tests were similar to those made during the L9-3 valve testing. The following instrumentation was eliminated from the L9-3 instrument list for the catch tank calibration.

<u>Instrument ID</u>	<u>Location</u>	<u>Range</u>
TE-PORV-2	Fluid temperature downstream of PORV	280-615K
TE-PORV-3	Fluid temperature downstream of PORV	280-615K
PE-PORV-1	Pressure upstream of PORV location	0-17.2 mPa
PE-PORV-2	Pressure downstream of PORV location	0-17.2 mPa
PDE-PORV	Differential pressure across PORV	0-13 mPa

The following instruments were added to the L9-3 instrumentation for the catch tank calibration.

<u>Instrument ID</u>	<u>Location</u>	<u>Range</u>
TE-CT-3	Fluid temperature upstream of flow control orifice	280-615K
PE-CT-3	Pressure upstream of flow control orifice	0-17.2 mPa

The reference orifice metering section was used for all of the catch tank calibration tests. The metering section was calibrated before the catch tank calibration testing was initiated and after the completion of the L9-3 valve tests. The Ballistic Calibrator at ARA III, used to calibrate the metering section is traceable to the National Bureau of Standards laboratories.

Warm-Up

Warm-up procedures were identical for the catch tank calibration and the L9-3 valve calibration. Due to the small restriction produced by the flow control orifice, warm-up flow through the test section was reduced and tolerance on loop isothermality was relaxed to ± 7 K.

Test Sequence and Procedures

Valve CV-5T was used to initiate the subcooled blowdown calibration tests. The test sequencing for the catch tank calibration was similar to

that for the subcooled, L9-3 valve calibration testing, and the flow paths were identical. Nitrogen pressurization was used in all but one test, BF-CTC-4, to maintain constant pressure, steady flow conditions. BF-CTC-4 was a transient subcooled test. Two nitrogen bottles were used to maintain pressure above saturation. The nitrogen bottles were at test initiation pressure prior to blowdown. As nitrogen was injected into the loop during the blowdown, the nitrogen pressure and loop pressure decreased, decreasing the mass flow rate and producing a transient test. The mass flow rates were similar to those expected for the saturated steam tests to be run in the L9-3 valve test series. The test was terminated when saturation pressure was reached.

Data Presentation

Steady State Results

Data from the seven steady state catch tank calibration data points are summarized in Table A-1. The orifice diameter is the diameter of the flow control orifice used for the test. Temperature is the average temperature through the test duration. Pressure is the mean pressure controlled during the test. \dot{M}_{LC} is the mass flow rate calculated from the load cells using a first order curve fit and differentiation technique. \dot{M}_{Ref} is the mass flow rate calculated from the reference mass flow orifice. $\Delta\dot{M}$ is the difference between the load cell mass flow rate and the reference mass flow rate in kg/s and %. The reference mass flow rate had an uncertainty of ± 0.02 kg/s, based on results of calibration prior to installation in the Blowdown facility.

These data indicate that the catch tank/load cell assembly was reading consistently higher than the reference and that lower mass flow rates produced higher % errors.

Transient Results

This section presents the data from the single transient catch tank calibration test run, BF-CTC-4. The data are presented in plots using

engineering units in Figures A1 through A12. Only those measurements that are necessary for qualification and assessment of load cell performance are reported.

The reference mass flow rate was calculated using data from the reference orifice metering section. The load cell mass flow rate was calculated by curve fitting the sum of the load cells and differentiating the curve fit. First to fifth order curve fits were applied to the load cell sum, with the best approximation by load cells to reference for the specified test duration being the third order fit. The third order fit resulted in mass flows approximately 5 to 7% higher than the reference which is in good agreement with the steady state tests (see Figure A1). The third order fit cannot, however, be construed as the most appropriate fit to use for transient tests in general.

This single test does not provide adequate information to assess the measurement and processing capability in a general sense. It can be said that in this particular case the method can be used to show that the load cell-catch tank assembly does respond effectively in determining mass flow rate for this transient blowdown. Additional testing and analytical evaluation is required in order to determine the overall effectiveness of the catch tank-load cell system in determining mass flow rates for transient tests, and in quantifying the uncertainty for such conditions.

Conclusions

At the initiation of the first L9-3 data point, an inadvertant valve opening caused a flex hose failure. Subsequent checks of load cell and catch tank system response during mass addition indicated that results of these calibration experiments were not valid for application to the L9-3 PORV calibration data. This pretest calibration, though not directly applicable for determination of the accuracy of the weighing system for the L9-3 test series, can be used to assess the transient response of the system in general. The method used to produce the transient tests is repeatable and can be effective in assessing transient responses under a variety of conditions. However, further catch tank calibration should be

considered prior to further use to assure that the measurement technique and data processing technique will yield acceptable uncertainty. The response of the catch tank was characterized by posttest calibration tests, and is documented in Reference A-3.

References

- A-1. Letter to R. S. Monson, System Operation Tests and Catch Tank Calibration for L9-3/4 Test Series, WAO-26-81.
- A-2. Drawing Number 415432, LTSF L9-3/4 Test Apparatus Assembly Released 12-9-81.
- A-3. Letter from W. A. Owca to T. F. Pointer, L9-3 Valve Sizing Test Summary, WAO-3-82, April 6, 1982.

APPENDIX B

UNCERTAINTY ANALYSIS



APPENDIX B

UNCERTAINTY ANALYSIS

This appendix describes the measurement uncertainty of the data taken during the L9-3 valve calibration tests. The stated uncertainty limits are given for a two sigma or 95% confidence level.

Each calculated uncertainty was divided into a signal component resulting from transducer and signal conditioning, and a data acquisition component resulting from acquisition electronics and recording equipment. Accuracy uncertainties are combined using the standard root sum square (RSS) technique for the percent of range (% Rg) uncertainty.

Data Acquisition System Uncertainty

The data acquisition system (DAS) and the voltage insertion calibration system contribute to the measurement uncertainty. The errors associated with the voltage calibration system are assumed to be less than the daily drift, measured at less than 0.05% of range. Stability of the bridge circuit power supply is better than 0.02% of range. Crosstalk contributes an uncertainty of 0.09% of range. Therefore, the total root sum square error attributed to the data acquisition system is 0.10% of range.

Transducer and Signal Conditioning Uncertainties

Temperature Measurements

Type K, grounded junction thermocouples and one Resistance Thermometer (RTD) were used during the L9-3 valve calibration testing. Reference B-1 quotes a 2.2 K uncertainty for an RTD.

Thermocouple uncertainties are tabulated in Table B-1. These are maximum uncertainties for the Type K thermocouples in the loop. The material uncertainty is from a manufacturers quote of ± 2.2 K at a 99%

confidence interval. This translates to ± 1.34 K at a 95% confidence interval. The drift, reference junction and polynomial approximation uncertainties are detailed in Reference B-1. The extension cable uncertainty is a Semiscale quote. The total uncertainty uses the root sum square (RSS) technique.

Pressure Measurements

Sources of error in the pressure transducers include hysteresis, nonlinearity, repeatability and inaccuracy of the excitation voltage. Coefficient drift and zero offset drift obtained from the VICAL data were negligible. Thermal effects were assumed to be negligible. Hysteresis, nonlinearity, and reproducibility were obtained from pretest calibration data. Error in the excitation voltage was assumed to be 0.05% of range. Individual pressure transducer uncertainties are summarized in Table B-2.

Differential Pressure Measurements

Table B-3 summarizes the uncertainty analysis associated with differential pressure measurements. Pressure sensitivity is the effect of absolute pressure on the differential pressure measurement, and was calculated using no flow, isothermal data taken during testing, by a method detailed in Reference B-2. Thermal effects were calculated from calibration data where available, and were estimated conservatively at 0.40% of reading where unavailable. The calibration laboratory uncertainty traceable to NBS standards is estimated at $\pm 0.02\%$ of range. Inaccuracy of the excitation voltage was estimated at $\pm 0.05\%$ of range. Nonlinearity, hysteresis, repeatability, and toggle were taken from calibration data. The total uncertainty was calculated using a root sum square (RSS) technique.

An uncertainty was not quoted for PDE-23 due to the unusual behavior of the transducer during blowdown. It was not used for accurate volume determination during testing but was used to track the volume depletion trend during tests.

Density Measurement Uncertainty

A two-beam gamma densitometer was used upstream of the PORV for a density measurement in the L9-3 valve calibration testing. The densitometer was not used for any calculations in determining mass flow rate. It was used to track density trends through the course of a blowdown and in determining the steam interval for the sizing tests. A detailed uncertainty analysis has not been done on the two-beam assembly. The densitometer uncertainty considered to be the 2σ difference between mean and actual density, has been estimated at ± 32 to 50 kg/m^3 .

Load Cell Uncertainty

The uncertainty of the load cell sum has been estimated at $\pm 1.0 \text{ kg}$,^{B-3} from calibration data and static load testing. This is not the uncertainty of the weighing system, but of the load cells only. The mass addition to the catch tank may not be accurately reflected by the load cells due to load sharing, transient response or other weighing system effects.

References

- B-1. G. D. Lassahn, LOFT Experimental Measurements Uncertainty Analysis Volume XIII Temperature Measurements, March 1982.
- B-2. G. D. Lassahn, LOFT Experimental Measurements Uncertainty Analysis Volume XII Differential Pressure Measurements, August 1981.
- B-3. G. E. Gruen, Letter to W. J. Quapp, Catch Tank Summary Report, GEG-26-80, September 8, 1980.

APPENDIX C

DATA PROCESSING AND QUALIFICATION

APPENDIX C

This section summarizes the methods used by the LTSF data system and the INEL Cyber system to produce the data tapes and plots presented in this report. The procedures used to qualify the data are also detailed.

DATA PROCESSING AND QUALIFICATION

The data was recorded at a rate of 50 samples/second on LTSF Mod Comp disk and transferred to digital tape after the test. The load cells were filtered at 1 and 10 Hz, all other data channels were filtered at 10 Hz and digitized with 16 bit resolution. The recorded voltage signals were converted to engineering units using a polynomial equation of the form:

$$\text{Measurement} = D_0 + D_1V + D_2V^2 + D_3V^3$$

where V is the original transducer voltage output and D_i are coefficients which depend on calibration data. Plots of the measurements, in engineering units, were then reviewed to determine the validity and success of each test.

At the end of each 8-hour shift, a voltage insertion calibration (VICAL) was performed. The VICAL is the method by which the data acquisition system is automatically calibrated by using a voltage insertion system to confirm measurement accuracy. This system, which is traceable to NBS standards, checks the zero offset, sensitivity variation, and linearity of each channel.

After the VICAL was recorded, the digital data tape was transferred to and processed on the INEL Cyber computer system. First, the data was reformatted to a form compatible with the CDC computer by using the program ZIPCON. The data was then converted from voltages to engineering units by using a polynomial expression (KALIB) similar to the expression used by the Mod Comp computer.

The data plots were then carefully analyzed and qualified to ensure the data's accuracy and integrity. The data plots returned from the Cyber computer were visually checked to make certain that they agreed with the data plots obtained from the Mod Comp computer. The procedure used to verify the consistency of the acquired data base was patterned after the technique developed for the LOFT Data Integrity Review Committee (DIRC). The data from pressure transducers in close proximity, such as PE-0-1 and PE-PORV-1, were compared to ensure that the two transducers corresponded to each other. The data were considered qualified if the two measurements agreed within the stated accuracy of ± 0.2 MPa and within a reasonable difference in pressure due to line friction losses.

Similarly, the data from two temperature transducers, TE-0-1 and TE-PORV-1, were compared to ensure that the two transducers agreed with each other. The data was considered qualified if the two measurements agreed within the stated accuracy of ± 3.1 K.

An additional consistency check involved the comparison of a pressure transducer with saturation pressure. The saturation pressure was calculated, using steam tables, from a thermocouple near the pressure tap.

Differential pressure transducers were compared to the pressure transducers throughout the system to maintain continuity in line pressure due to friction losses and to track flow rate trends during depressurization. The liquid level measurement was compared to the expected volume decrease in the pressure vessel.

The densitometer was compared to steam table data using appropriate pressure and temperature and was considered qualified if agreement was within $\pm 50\%$ kg/m^3 .

The load cell data was considered qualified if the general trend of mass addition to the catch tank was detectable, if upstream pressure changes were reflected in an altered mass flow rate, and if the load cell sum and resultant mass flow rate were reasonable and consistent. The load cell calibration coefficients used during testing were based on an assumed

10 V calibration excitation voltage when an actual 11.028 excitation had been used. The data presented here has been processed with corrected calibration coefficients.

APPENDIX D

DATA ACQUISITION SYSTEM

APPENDIX D

DATA ACQUISITION SYSTEM

This appendix briefly describes the main components and capabilities of the Data Acquisition System at the LOFT Test Support Facility. Additional detailed information can be found in Reference C-1.

The LTSF data acquisition system, as presently configured, acquires experimental and operational test data from the blowdown facility (BF) and two-phase flow loop test assemblies located at TAN 641. Operational test data is amplified and routed to digital panel meters located in the control rooms to provide online display of information necessary for controlling and operating the test loops. This information is low bandwidth or steady-state.

Higher bandwidth, or transient experimental data, is routed concurrently to the Neff 620 Analog Input Subsystem for permanent recording for further data analysis. The input patch panels provide the signal programming capabilities. The narrow band digital, or Neff 620 System, which was used for the L9-3 tests, provides the capability for recording up to 256 channels of relatively low bandwidth (dc-10 Hz) analog information.

The Narrow-Band Digital Data Acquisition and Processing System includes:

- o Neff 620 Series 300 Signal Conditioners
- o Neff 620 Series 100 Analog Input Subsystem
- o Mod Comp II/45 Central Processor
- o Keyboard--Printer
- o Digital Magnetic Tape Recorder

- o Two CRT Terminals with Hard Copy Units
- o 25 MWord Moving Head Disc
- o Voltage Insertion Calibration Source
- o Time Code Translator/Generator
- o Tape Search Unit
- o Card Reader.

These components are configured to form a complete digital data acquisition system with data processing, storage, and presentation capabilities. Millivolt signals from the transducers are conditioned by the Neff 620 Series 300 Signal Conditioners and routed to the input patch panel. This equipment provides both constant voltage and constant current excitation for bridge type transducers. Signals from thermocouples and special signal conditioners are directly connected to the input patch panel.

Signals are patched to the desired channel on the Neff 620 Series 100 Analog Input Subsystem where they are amplified, filtered, time-division multiplexed, and converted from analog to digital information for subsequent storage on magnetic disc or digital tape. The Mod Comp II/45 is the control processor for the system and, through program instructions manipulates and processes incoming data for storage on magnetic disc or digital tape, program instructions are entered by the operator from the keyboard printer and refreshed CRT terminal. A storage type CRT terminal is used to make engineering unit versus time graphic data plots of all test data after the test has been performed.

The main individual components are described in the following paragraphs.

Neff 620 Series 300 Signal Conditioner. The Neff Series 300 Signal Conditioner is a data acquisition subsystem that conditions the output of

signal transducers to be compatible with analog measuring systems. The system contains 44 channels. Each channel can be individually configured for a particular transducer type. These conditions are used to condition bridge-type transducers such as pressure transducers and RTD for the LTSF Data Acquisition System. The subsystem provides constant current or constant voltage excitation, bridge completion and programmable calibration.

Analog Input Subsystem. The Neff System 620 Series 100 Analog Input Subsystem is a system that converts low-level and high-level analog input signals to digital form for processing by a digital computer. The system provides the required signal amplification, filtering and multiplexing for up to 256 channels at through-put rates to 50 kHz. Each channel is equipped with a separate guarded differential input preamplifier followed by an active low-pass filter. Preamplifier gain and filter bandwidth are selected by plug in modules. Low-level preamplifier gains of 10, 20, 50, and 100 are provided. High-level preamplifier gain modules with 1 and 10 gains are available. Filter modules with bandwidths of 1, 10, 100, 500, and 1000 Hz are provided. The filters are high-level active low-pass type with 2-pole Butterworth response. The filter serves to prevent aliasing errors and reduces system noise.

Central Processor. The Mod Comp II/45 is used as the central processor for the system. It is a 800 nanosecond memory cycle time, 16-bit digital computer supplied with 64 K words of core memory. The machine has a large instruction set and is designed to be efficient in executing higher level software, including real time multiprogramming systems, discs operating systems, and interactive language systems. The processor has a memory protect and parity check feature and is equipped with four direct memory access ports so the computer can be used in a data acquisition mode without CPU intervention.

Moving Head Disk. An Amplex Model DM323 Moving Head Disk provides storage capacity up to 24,000,000 words and data transfer rates of up to 150,000 words/second. The device uses a removable 20 surface disk pack.

Voltage Insertion Calibration System. Each channel of the Data Acquisition System can be calibrated either manually or automatically under computer control. During calibration the input of each Neff 620 System Preamplifier is switched from the normal data signal input to a common calibration input. The calibration voltages are derived from a High Speed Digitally Programmable dc voltage standard manufactured by Electronics Development Corporation. This voltage standard is controlled by the Mod Comp II/45 computer. The voltages can be programmed from -9.999 to +9.999 V dc with a resolution of 10 μ V or 1 ppm on the 100 millivolt full scale range. The accuracy of the unit is $\pm 0.005\%$ of programmed value and $\pm 0.005\%$ of range +5% μ volts. These accuracies are traceable through a bank of saturated standard cells to the National Bureau of Standards Laboratories. The reference voltage is derived from an aged temperature compensated Zener diode.

Timing Systems. The time reference is generated from a 3 MHz reference oscillator which has a drift rate of less than one part in 10^9 ; this corresponds to a time error of less than 50 microseconds each day. The generator can be synchronized to an external time standard such as radio station WWV when an accurate real time reference is required.

Reference

- D-1. B. O. Meng, LOFT Test Support Facility Data Acquisition System Description, LOFT Technical Report, ltr-10-59, December 12, 1978.

TABLE 1. L9-3 EXPERIMENTAL PORV TEST INSTRUMENTATION

Instrument Identification	Description	Range
TE-5	Fluid temperature in pressure vessel	280-615 K
TE-SB-2	Fluid temperature in 14-in. spool, away from pressure vessel	280-615 K
TE-0-1	Fluid temperature upstream of reference mass flow orifice	280-615 K
TE-PORV-1	Fluid temperature upstream of PORV	280-615 K
TE-PORV-2	Fluid temperature downstream of PORV	280-615 K
PE-3	Pressure in the pressure vessel	0-20.7 MPa
PE-SB-2	Pressure in the 14-in. spool	0-17.2 MPa
PE-0-1	Pressure upstream of the reference mass flow orifice	0-17.2 MPa
PE-PORV-1	Pressure upstream of the PORV	0-17.2 MPa
PE-PORV-2	Pressure downstream of the PORV	0-17.2 MPa
PE-N-1	Pressure of nitrogen supply	0-17.2 MPa
PDE-23	Liquid level in pressure vessel	0-300 cm
PDE-FT-1	Differential pressure across reference mass flow orifice	0-25 kPa 0-125 kPa 0-344 kPa
PDE-REF	Differential pressure from the downstream reference orifice flange to PE-PORV-1	0-40 kPa
PDE-PORV	Differential pressure across the PORV	0-10.3 MPa
PDE-FCO	Differential pressure across a flow control orifice (used for catch tank calibration only)	0-10 MPa
DE-1A	Densitometer upstream of PORV	0-1000 kg/m ³
DE-1B	Densitometer upstream of PORV	0-1000 kg/m ³
LD-LC-1	Load Cell 1	0-2800 kg
LD-LC-2	Load Cell 2	0-2800 kg

TABLE B-1. TEMPERATURE MEASUREMENT UNCERTAINTY

Type K thermocouple uncertainty

Material	± 1.34 K
Drift	$\pm 0.2\%$ Rd = ± 1.2 K max
Reference junction	± 0.4 K
Polynomial approximation	± 2.0 K
Extension cable	± 1.25 K
DAS	$\pm 0.1\%$ Rg = ± 0.6 K

Total uncertainty = ± 3.05 K

The above total uncertainty is applicable to the following measurements:

TE-0-1

TE-PORV-1

TE-PORV-2

TE-SB-2

TE-5 is a Resistance Thermometer (RTD) with a quoted uncertainty of ± 2.2 K

TABLE 2. L9-3 EXPERIMENTAL PORV TEST DATA SUMMARY

Test Identification	Test Type (SC/SAT)	Valve Setting (H/L)	Valve Opening (%)	Test Initiation Conditions				Test Conditions During Flow	
				TE-5 (K)	TE-PORV-1 (K)	PE-3 (MPa)	PE-PORV-1 (MPa)	P-Range (MPa)	T-Range (K)
BF-L9-3-1B	SAT	L	19.9	612	611	15.5	15.5	6.4-10.0	553-584
-1C	SAT	L	22.8	611	612	15.7	15.7	5.3-10.2	541-586
-1D	SAT	L	25.3	609	609	15.6	15.6	5.1-9.3	538-579
-1E	SAT	L	24.0	610	611	15.6	15.7	6.0-8.8	548-575
-1ER	SAT	L	24.0	609	608	15.2	15.2	6.1-9.4	550-580
-2A	SAT	H	100.0	589	589	15.6	15.5	3.0-4.6	507-532
-2B	SAT	H	37.0	597	598	15.0	15.0	4.5-8.3	555-571
-2C	SAT	H	50.5	607	609	15.5	15.5	3.8-8.0	520-568
-2D	SAT	H	65.8	611	612	15.6	15.6	3.7-7.7	519-565
-2E	SAT	H	81.8	608	609	15.5	15.5	3.6-6.6	517-555
-2F	SAT	H	60.8	610	611	15.8	15.7	3.5-7.0	516-559
-2G	SAT	H	55.0	609	609	15.7	15.8	4.2-8.0	526-568
-2H	SAT	H	52.2	609	609	15.5	15.5	4.0-8.0	523-568
-2HRR	SAT	H	52.2	610	611	15.5	15.5	3.6-8.4	517-572
BF-L9-3-SC-1	SC	H	52.2	587	589	11.1	11.1	10.8	586
SC-2	SC	H	52.2	581	578	10.9	10.9	10.7	578
SC-3	SC	H	52.2	571	573	11.1	11.1	10.7	571
SC-4R	SC	H	52.2	561	560	10.9	10.9	10.7	558

TABLE A-1. CATCH TANK CALIBRATION TEST DATA SUMMARY

Test Identification	Orifice Diameter (cm)	Temperature (K)	Pressure (MPa)	\dot{M}_{LC} (kg/s)	\dot{M}_{Ref} (kg/s)	$\Delta \dot{M}$ (kg/s)	$\Delta \dot{M}$ (%)
BF-CTC-1	0.541	550±2.0	6.9±.10	1.79	1.68±0.02	+0.11	6.5
BF-CTC-2	0.541	546±2.0	6.9±0.06	1.85	1.74±0.02	+0.11	6.3
BF-CTC-3	0.541	540±2.0	7.0±0.06	1.93	1.76±0.02	+0.17	9.7
BF-CTC-5	0.279	590±2.0	12.0±0.08	0.51	0.43±0.02	+0.08	18.6
BF-CTC-6	0.279	583±1.0	11.9±0.10	0.49	0.44±0.02	+0.05	11.4
BF-CTC-7	0.279	574±1.0	11.0-12.0 ^a	0.47	0.40±0.02	+0.07	17.5
BF-CTC-7R	0.279	578±1.0	11.9±0.05	0.49	0.46±0.02	+0.03	6.5

a. The nitrogen control valve did not function.

TABLE B-2. ABSOLUTE PRESSURE MEASUREMENT UNCERTAINTY

Transducer Identification Range/ Uncertainty Factor	PE-3 0-20.7 MPa	PE-N-1 0-17.2 MPa	PE-O-1 0-17.2 MPa	PE-PORV-1 0-17.2 MPa	PE-PORV-2 0-17.2 MPa	PE-SB-2 0-17.2 MPa
Hysteresis (% Rg)	0.06	0.03	0.15	0.12	0.10	0.06
Nonlinearity (% Rg)	0.22	0.21	0.26	0.19	0.18	0.22
Repeatability (% Rg)	0.02	0.01	0.03	0.02	0.02	0.02
Excitation voltage (% Rg)	0.05	0.05	0.05	0.05	0.05	0.05
DAS (% Rg)	0.1	0.10	0.10	0.10	0.10	0.10
Total Uncertainty (% Rg)	0.25	0.24	0.33	0.25	0.23	0.25
Total Uncertainty (MPa)	= 0.04	= 0.04	= 0.05	= 0.04	= 0.04	= 0.04

TABLE B-3. DIFFERENTIAL PRESSURE MEASUREMENT UNCERTAINTY

Transducer Identification Range/ Uncertainty Factor	PDE-FI-1 (12.5 kPa)	PDE-FI-1 (125 kPa)	PDE-FI-1 (344 kPa)	PDE-REF (50 kPa)	PDE-PORV (13.0 MPa)	PDE-FCO (10.34 MPa)
Pressure sensitivity (% Rg)	0.40	0.74	0.36	0.76	0.23	0.11
Thermal effects (% Rg)	0.40	0.40	0.40	0.40	0.28	0.11
Calibration data (% Rg)	0.02	0.02	0.02	0.02	0.02	0.02
Excitation voltage (% Rg)	0.05	0.05	0.05	0.05	0.05	0.05
Nonlinearity (% Rg)	0.50	0.33	0.25	0.31	0.56	0.17
Hysteresis (% Rg)	0.08	0.20	0.25	0.21	0.20	0.05
Repeatability (% Rg)	0.02	0.23	0.15	0.05	0.04	0.02
Toggle (% Rg)	0.59	1.06	0.18	0.12	0.13	0.14
DAS (% Rg)	<u>0.10</u>	<u>0.10</u>	<u>0.10</u>	<u>0.10</u>	<u>0.10</u>	<u>0.10</u>
Total uncertainty (% Rg)	0.97	1.43	0.70	0.95	0.72	0.30
Total uncertainty (kPa)	0.12	0.18	2.41	0.48	93.6	31.02